Journal
ofOrgano
metallic
Chemistry

ELSEVIER

Synthesis, magnetic susceptibility and X-ray crystal structure of (^{t}BuNCHCHN^{t}Bu)$_3$Yb

Mikhail N. Bochkarev [a], Alexander A. Trifonov [a], F. Geoffrey N. Cloke [b],
Christopher I. Dalby [b], Phillip T. Matsunaga [c], Richard A. Andersen [c], Herbert Schumann [d,*],
Jörg Loebel [d], Holger Hemling [d]

[a] *Institute of Organometallic Chemistry, Academy of Sciences of Russia, Tropinina 49, Nizhny Novgorod, Russian Federation*
[b] *School of Chemistry and Molecular Sciences, University of Sussex, Brighton BN1 9QJ, UK*
[c] *Chemistry Department and Materials and Molecular Research Division of Lawrence Berkeley Laboratory, University of California,
Berkeley CA 94720, USA*
[d] *Institut für Anorganische und Analytische Chemie der Technischen Universität Berlin, Straße des 17. Juni 135, D-10623 Berlin, Germany*

Abstract

The reaction of $(C_{10}H_8)Yb(THF)_3$ with ^{t}BuN=CHCH=N^{t}Bu (^{t}Budad) in tetrahydrofuran at room temperature leads to Yb(^{t}Budad)$_3$ (1), which is also obtained from the reaction of YbCl$_3$ and three molar equivalents of K(^{t}Budad) in tetrahydrofuran or by metal vapor synthesis. 1 has been characterized by X-ray diffraction. The crystals are monoclinic, space group $C2$, $Z = 2$ with $a = 1034.8(9)$, $b = 1710.4(6)$, $c = 1020.4(8)$ pm, $\beta = 113.28(2)°$. The structure was refined to $R = 0.0274$ for 1466 observed reflections ($F_O > 4\sigma(F_O)$). The structure shows that the empirical composition is Yb(^{t}Budad)$_3$ and that the coordination number of Yb is six, but the X-ray data are not sufficiently accurate to judge if the oxidation state of ytterbium is zero, two or three. The magnetic susceptibility of solid 1, prepared by metal vapor synthesis, was studied from 5 to 300 K. The magnetic results are explained by postulating that the bivalent ytterbium species [Yb^{II}(^{t}Budad$^-$)$_2$(^{t}Budad)] predominates at low temperature and as the temperature increases the trivalent ytterbium species [Yb^{III}(^{t}Budad$^-$)$_3$] predominates in the solid state.

1. Introduction

The diazabutadiene ligands R–N=CH–CH=N–R (abbreviated as Rdad) have already been shown to stabilize low formal oxidation states of d-transition metals [1]. The homoleptic diazabutadiene complexes of Ytterbium and the lanthanides Nd, Sm and Yb, Ln(^{t}Budad)$_3$ have been obtained by metal vapor synthesis techniques and have been described as Ln^0 complexes on the basis of NMR and IR spectroscopic investigations [2]. However attempts to obtain crystals of these complexes good enough for an X-ray crystal structure determination did not succeed. Recently some of us reported the synthesis of Yb(^{t}Budad)$_2$, which was characterized by elemental analysis, ESR and IR spec-

tra [3]. During the attempts to reproduce these results and to get more detailed information about the structure of this compound, Yb(^{t}Budad)$_3$ (1) was isolated. The compounds isolated by each synthesis technique gave identical analyses showing that they have identical empirical compositions. Here we describe new syntheses, magnetic susceptibility studies, and the X-ray structural investigation of this interesting compound.

2. Results and discussion

The substitution of the naphthalene ligand in $(C_{10}H_8)Yb(THF)_3$ (2) [4] by ^{t}Budad and the interaction of YbCl$_3$ with K$^+$[^{t}Budad]$^-$ were proposed as possible routes for the synthesis of Yb(^{t}Budad)$_3$ (1). The latter one is well known as the preparative route to numerous diazabutadiene complexes of d-transition
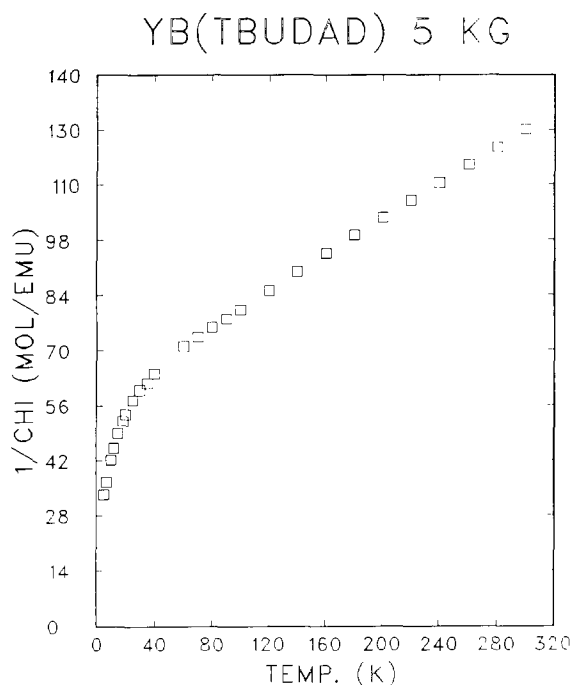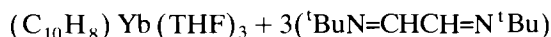
---

* Corresponding author.

YB(TBUDAD) 5 KG

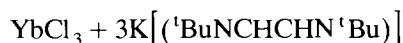Fig. 1. Magnetic susceptibility of solid **1** as a function of temperature [K].

metals [5–11]. It was shown that both methods proceed easily at room temperature to yield **1** in high yields (Eqs. (1) and (2)). A compound of identical chemical and physical properties was obtained by allowing ytterbium vapor to interact with the diazadiene at cryogenic temperatures (77 K, Eq. (3)).
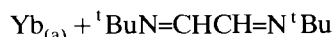
$$(C_{10}H_8) \, Yb \, (THF)_3 + 3('BuN=CHCH=N'Bu)$$

$$\mathbf{2}$$

$$\xrightarrow[\text{2h,20°C}]{\text{THF}} Yb('BuNCHCHN'Bu)_3 + C_{10}H_8 \qquad (1)$$

$$\mathbf{1}$$

$$YbCl_3 + 3K[('BuNCHCHN'Bu)]$$

$$\xrightarrow[\text{10h,20°C}]{\text{THF}} Yb('BuNCHCHN'Bu)_3 + 3KCl \qquad (2)$$

$$\mathbf{1}$$

$$Yb_{(a)} + 'BuN=CHCH=N'Bu$$

$$\xrightarrow{\text{77 K}} Yb('BuNCHCHN'Bu)_3 \qquad (3)$$

$$\mathbf{1}$$

1 is a deep green, air- and moisture-sensitive crystalline solid, which melts at 194 to 198°C with decomposition. It is paramagnetic in the solid state. The plot of χ_M^{-1} as a function of temperature is non-linear at 5 kGauss and at 40 kGauss, applied magnetic field (Fig. 1). The curve at 5 kGauss is essentially superimposable upon that at 40 kGauss. The curved line may be separated into three regions, based upon a tempera-

ture range, for the purposes of discussion. At the high temperature range (80–300 K) χ_M^{-1} is linear in temperature, satisfying the Curie-Weiss Law, $\chi_M^{-1} = (T-\theta) (C)^{-1}$. The slope of the plot χ_M^{-1} as a function of temperature gives C^{-1}, from which the magnetic moment can be calculated since $\mu = 2.828 \, C^{1/2}$. The magnetic moment over the high temperature range is 5.91 Bohr magnetons (BM) at 5 kGauss and 5.78 B.M. at 40 kGauss. In each case θ (the extrapolated intercept) is large, -252 and -231 K, respectively. This large value shows that χ_M^{-1} does not go to zero as the absolute temperature approaches zero, and that the compound does not behave as a simple isolated paramagnet.

At low temperature (5–15 K) the slope of χ_M^{-1} is also linear in temperature with the value of $\mu = 2.30$ BM and 2.34 BM at 5 and 40 kGauss, respectively. The values of θ are -14 and -16 K, respectively. Only five data points were measured at each magnetic field so the error associated with each datum is relatively large. However, there is no doubt that the magnetic moment is substantially reduced from that measured at high temperature. The intermediate temperature range (15 to 80 K) gives a curve that is non-linear and probably reflects the changing population of at least two species and their individual magnetic moments, i.e., the observed curve reflects the weighted superposition of two or more curves due to two or more magnetic species.

A microscopic explanation can be developed that accounts for the magnetic behavior. For simplicity, two species, A and B, will be postulated to be present in the solid state in amounts that change with temperature. At high temperature, species A predominates with a magnetic moment of ca. 6 BM. At low temperature, B predominates with a magnetic moment of ca. 2.3 BM. In the intermediate temperature range varying amounts of A and B are present and the weighted average of their magnetic susceptibility gives the non-linear behavior.

In the case of ytterbium, Yb^{II} is diamagnetic and Yb^{III} is paramagnetic with an electron configuration of $4f^{13}$. In the free ion the term symbol is $^2F_{7/2}$. The ground state has $J = 7/2$ and the first excited state has $J = 5/2$ which is about 1000 cm^{-1} above the ground state (at 300 K, $kT = 208$ cm^{-1}). At low temperature all of the molecules are in the $J = 7/2$ state and as the temperature increases, there will be an admixture of the $J = 5/2$ state into the ground state [12]. Thus, for Yb^{III} compounds that behave as isolated paramagnets, a plot of χ_M^{-1} as a function of the absolute temperature is linear at low temperature with a magnetic moment of ca. 4.2 BM and linear at high temperature with a magnetic moment of ca. 4.8 BM. At intermediate temperatures the curve is non-linear, reflecting the weighted average of the $J = 7/2$ and $J = 5/2$ states. This explanation has been used qualitatively to ratio-

nalize the χ_M^{-1} vs. T plot for a variety of organometallic ytterbium^{III} compounds [13]. This explanation cannot explain the magnetic behavior of the Yb(^{t}Budad)$_3$ compound, where A is the species with $J = 5/2$ and B is the species with $J = 7/2$ because the observed low temperature magnetic moment of ca. 2.3 BM is far too low. Furthermore, if this were true the magnetic moment should decrease with the population of the $J = 5/2$ state which increases with temperature.

Another possible explanation is to postulate that A is a Yb^{III} species and B is a Yb^{II} species and that these species are in equilibrium in the solid state. If A is a Yb^{III} species, then there are two ways that the negative charge can be redistributed over the three ^{t}BuNCHC-HN^{t}Bu ligands; (a) three radical anions, (^{t}Budad$^-$); or (b) a dianion and a radical anion (^{t}Budad^{2-}) (^{t}Budad$^-$)(^{t}Budad). In (a) the observed magnetic moment is expected to be the root-mean-square sum of the individual magnetic moments, $[(4.2)^2 + (1.73)^2 + 1.73)^2 + (1.73)^2]^{1/2}$ or 5.5 BM. If (b), then the expected magnetic moment is $[(4.2)^2 + (1.73)^2]^{1/2}$ or 4.8 BM, this assumes that dad^{2-} is diamagnetic. If B is Yb^{II}, then there are again two ways to distribute the two negative charges among the three dad ligands, (a) (^{t}Budad$^-$)$_2$ (^{t}Budad); or (b) (^{t}Budad^{2-})(^{t}Budad). In these cases the expected magnetic moment (assuming no interactions between the spins) is $[(1.73)^2 + (1.73)^2]^{1/2}$ or 2.4 BM in the case of (a) and zero for the diamagnetic case (b). This last explanation qualitatively fits the experimental data. At low temperature, the predominant species is bivalent ytterbium, Yb^{II}(^{t}Budad$^-$)$_2$(^{t}Budad), and at high temperature the predominant species is trivalent ytterbium, Yb^{III}(^{t}Budad$^-$)$_3$.
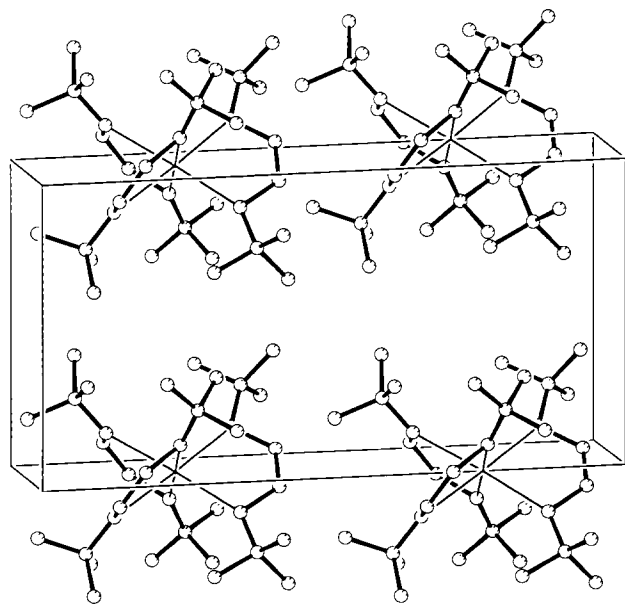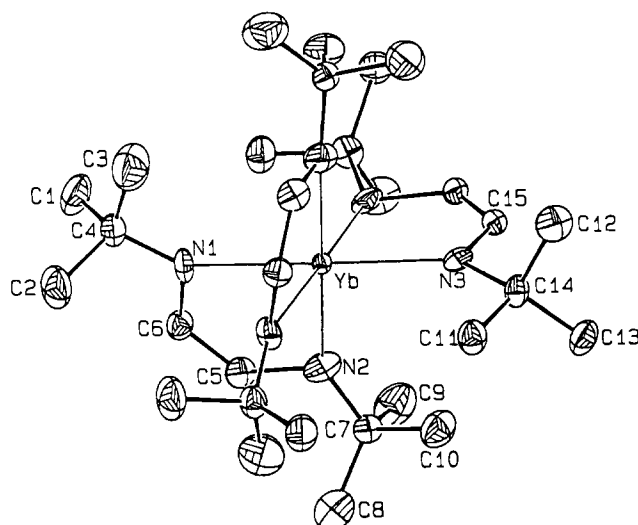

Fig. 2. PLUTON plot [14] of the unit cell of 1.

Fig. 3. ORTEP drawing [15] of 1, with the numbering scheme. Thermal ellipsoids scaled at 50% probability level. The symmetry operation to produce the missing positions is $- x, y, - z$.

This postulate is reasonable since at low temperature bivalent ytterbium is the ground state and the compound is stabilized by the Coulombic attraction between the metal center and the radical anions. Oxidation of Yb^{II} to Yb^{III} is an endothermic process that must be compensated by the Coulombic attraction between the trivalent metal center and the radical anions which is favorable only at temperatures greater than ca. 80 K.

The magnetic susceptibility data also rule out the formation of Yb^0(dad)$_3$ since Yb^0 has an electronic configuration of 4f^{14}6s^2 which presumably is diamagnetic, thus the compound should be diamagnetic in the ground state. The magnetic data do not, however, rule out the possibility that some Yb^0 species are present, though this seems unlikely to us.

The X-ray crystal structure of the green crystals of 1 shows two molecules in the unit cell (Fig. 2) with molecules in a distorted tetragonal bipyramid formed by six nitrogen atoms of the (^{t}Budad) ligands around the six coordinate Yb atom in the center (Fig. 3). The interplanar angle between the planes [N(1)–N(1$^#$)–N(3)–N(3$^#$)] and [N(2)–N(1$^#$)–N(2$^#$)–N(3$^#$)] is 72.21(51)°, where the ytterbium atom is directly located in both (deviation 0.0 and 4.3 pm, respectively). The bite angles N(1)–Yb–N(2) and N(3)–Yb–N(3$^#$) are 83(2)° and 84(3)°, respectively. The Yb–N distances, 243(4) pm for Yb–N(1), 240.3(14) pm for Yb–N(2) and 240(5) pm for Yb–N(3) are in between the bond lengths in coordinative N–Ln bonds as in Lu(C$_6$H$_4$CH$_2$NMe$_2$)$_3$ (246.8 to 258.8) [16] and in Ln–N bonds as in (C$_5$Me$_5$)$_2$ Y–N(SiMe$_3$)$_2$ (225.3 and 227.4) [17] or [Li(THF)$_4$][(C$_5$-H$_5$)$_2$Lu(NPh$_2$)$_2$] (229.0 and 229.3) [18]. The distances correspond very well with the Yb–N bond lengths in Na[Yb{N(SiMe$_3$)$_2$}$_3$] (246 pm) [19] and [Yb{N(Si-

Me$_3$)$_2$}$_2$][AlMe$_3$]$_2$ (251.0 and 257.3 pm [20]) with bridging bis(trimethylsilyl)amido groups. The chelating (^{t}Budad) ligands coordinate to the Yb atom forming three five-membered metallacycles with the central Yb atom in the [N(3)–C(15)–C(15$^\#$)–N(3$^\#$)] plane (deviation 0.0 pm), but not exactly in the [N(1)–C(6)–C(5)–N(2)] plane [deviation 5.1(14) pm].

The most remarkable feature of the structure is the bonding lengths within the (^{t}Budad) ligands. All three ligands should be radical anions after accepting one electron each from ytterbium with delocalized double bonds in the N–C–C–N skeleton [1,21]. Indeed the bonds C(5)–C(6) (139 pm) and C(15)–C(15$^\#$) (135 pm) show double bond character with the shortest contact within the planar metallacycle Yb–N(3)–C15–C(15$^\#$)–N(3$^\#$). But astonishingly there is a distortion in this NCCN skeleton for both ligands of −12.6° and −12.9°. The N–C distances (151 pm for N(2)–C(5) up to 161 pm for N(1)–C(6)) are significantly longer than the N=C double bonds in the free ligand (128.3 pm [22]) and the N–C single bonds in Li[Ho(NMe(CH$_2$)$_2$-NMe$_2$)$_4$] (144.4 to 148.3 pm [23]). They come close to the sum of the covalent radii of carbon and nitrogen (151 pm [24]). A comparable fixation of the double bond in the center of the (Rdad) ligand is found in complexes with (Rdad)$^{2-}$, e.g. in Ta(OAr)$_3$[Ar-NC(CH$_2$Ph)=C(CH$_2$Ph)NAr] (d(C=C): 135 pm, d(N–C) 143 pm [25] and in Ga(^{t}Budad)$_2$(d(C=C) 135.0 pm, d(N–C) 139.5 pm [26]).

The room temperature X-ray crystallographic result and the higher temperature magnetic susceptibility result are consistent with the formulation Yb^{III}-(^{t}Budad$^-$)$_3$. The susceptibility results are best interpreted by assuming that the Yb^{III} center (4f^{13} electron configuration) and the three dad radical anions spins do not couple. At low temperature the magnetic result suggests that the bivalent formulation [Yb^{II}(^{t}Budad$^-$)$_2$(^{t}Budad)] is more stable, and this is the ground electronic state of this molecule.

3. Experimental section

All operations were carried out under vacuum or dry argon using standard Schlenk techniques. Solvents were dried and deoxygenated by refluxing over sodium ketyl. The IR spectra were recorded on a Perkin-Elmer 577 spectrophotometer.

3.1. Tris(di-tert-butyl diazadiene)ytterbium(III) (1)

Method 1: 1.31 g (2.53 mmol) of (C$_{10}$H$_8$)Yb(THF)$_3$ (2) was added slowly to a solution of 1.28 g (7.61 mmol) of (^{t}Budad) in 30 ml of THF at room temperature. The reaction mixture was stirred for 2 h. A green solution is formed after dissolution of 2. Evaporation of THF in

vacuo and recrystallization of the residue from toluene yields 1.37 g (80%) 1; m.p.: 194–198°C (with decomp.). In the mother liquor 0.29 g (92%) of naphthalene was found by GLC. IR (Nujol): 2970, 1635, 1475, 1360, 1310, 1240, 1210, 1155, 985, 750 cm^{-1}. Anal. Found: C, 53.12; H, 8.75; N, 12.09; Yb, 25.54. C$_{30}$H$_{60}$N$_6$Yb (1) calc.: C, 53.19; H, 8.92; N, 12.40; Yb, 25.53%.

Method 2: 30 ml of a solution of [K$^+$][(^{t}Budad)$^-$] in THF, obtained by the reaction of 1.96 g (11.60 mmol) of (^{t}Budad) with 0.46 g (11.67 mmol) of K was added slowly to a suspension of 1.09 g (3.89 mmol) of YbCl$_3$ in 30 ml of THF. The reaction mixture was stirred for 10 h at room temperature, the solution was decanted and filtered from solid precipitates, THF was evaporated in vacuo and the residue recrystallized from a toluene : hexane 1 : 1 mixture. The green crystals of 1 were washed with cold hexane and dried in vacuo. Yield: 1.89 g (72%).

Method 3: Cocondensation of ytterbium vapor (1.70 g, 10 mmol) generated from a resistively heated alumina crucible with an excess of ^{t}Budad (29.42 g, 175 mmol) at 77 K over a period of 3 h yielded a deep green matrix. After warm-up under dinitrogen, the product was extracted from the reactor with toluene (750 ml) and immediately filtered on Celite on a glass

Table 1

Crystal and data collection parameters for (^{t}Budad)$_3$Yb [a]

Empirical formula	C$_{30}$H$_{60}$N$_6$Yb
Formula weight	677.88
Temperature	139(2) K
Wavelength	.71069 Å
Crystal system	monoclinic
Space group	C2
Unit cell dimensions	$a = 1034.8(9)$pm,
	$b = 1710.4(6)$pm,
	$c = 1020.4(8)$pm.
	$\beta = 113.28(2)°$,
Volume	1659(2) Å^3
Z	2
Density (calculated)	1.357 g cm^{-3}
Absorption coefficient	2.845 mm^{-1}
F(000)	704
Crystal size	0.33 × 0.20 × 0.05 mm
Theta range for data collection	2.17 to 25.00
Index ranges	−12 ≤ h ≤ 11, 0 ≤ k ≤ 20,
	0 ≤ l ≤ 12
Reflections collected	1606
Independent reflections	1516 [R(int) = 0.0192]
Refinement method	Full-matrix least-squares on F^2
Data/restraints/parameters	1466/1/168
Goodness-of-fit on F^2	1.142
Final R indices [$I > 4\sigma(I)$]	R1 = 0.0274, wR2 = 0.0688
R indices (all data 1516)	R1 = 0.0306, wR2 = 0.0816
Absolute structure parameter	0.06(7)
Largest diff. peak and hole	1.100 and −0.602

[a] Estimated standard deviations of the last significant digit are given in parentheses.

Table 2
Atomic coordinates ($\times 10^4$) and displacement parameters ($\text{Å}^2 \times 10^3$) for 1. U(eq) as one third of the trace of the orthogonalized U_{ij} tensor

Atom	x	y	z	U_{eq}
Yb	0	2454(2)	0	21(1)
C(1)	−3093(45)	4020(20)	−3718(31)	81(11)
C(2)	−1647(41)	4904(15)	−1839(36)	83(10)
C(3)	−527(36)	3935(23)	−2873(38)	87(11)
C(4)	−1699(25)	4086(13)	−2427(24)	45(5)
N(1)	−1337(58)	3576(26)	−1298(53)	44(11)
C(5)	−2725(20)	3104(14)	260(22)	45(5)
C(6)	−2670(22)	3550(13)	−854(21)	43(5)
N(2)	−1715(16)	2465(38)	1043(14)	50(5)
C(7)	−2012(19)	2176(12)	2182(21)	36(4)
C(8)	−2438(39)	2723(19)	3102(32)	89(12)
C(9)	−3118(37)	1565(21)	1564(35)	88(11)
C(10)	−639(28)	1784(18)	3106(28)	65(7)
C(11)	3183(27)	1955(14)	3249(26)	57(6)
C(12)	3676(23)	792(19)	2084(27)	63(7)
C(13)	2390(37)	642(18)	3638(28)	63(7)
C(14)	2603(22)	1189(13)	2552(23)	44(5)
N(3)	1524(59)	1416(29)	1296(43)	44(11)
C(15)	612(20)	699(10)	584(19)	32(4)

solution, containing some crystals of 1 was dropped into a device similar to that reported by Veith and Bärninghausen [27]. A green crystal of dimensions $0.325 \times 0.200 \times 0.050$ mm^2 was selected, glued on the top of a glass fiber and transferred onto a goniometer

frit to remove unreacted metal. The resultant deep green solution was stripped to dryness in vacuo and the excess ^{t}Budad removed by sublimation ($50°\text{C}/10^{-4}$ mbar). The residue was extracted with hexane (3×150 ml), filtered on Celite on a glass frit, and the filtrate concentrated in vacuo to ca. 150 ml. Slow cooling to −20°C afforded deep green microcrystals of the product, yield 2.90 g (43% based on Yb). IR (Nujol): 1460 cm^{-1} (νCN); ^{1}H NMR (C$_6$D$_6$, 500 MHz): δ 9.48 (s, Me$_3$C). Anal. Found: C, 53.36; H, 8.61; N, 12.24. C$_{30}$H$_{60}$N$_6$Yb (1) calc.: C, 53.19; H, 8.92; N, 12.40%.

3.2. X-Ray crystal structure determination

Suitable crystals of 1 were obtained by recrystallization from toluene. A small amount of the toluene

Table 3
Bond lengths [Å]. Symmetry transformations used to generate equivalent atoms: ($^\#$: −x, y, −z)

Bond	Distance	Atom	Distance
Yb–N(3$^\#$)	2.40(5)	Yb–N(3)	2.40(5)
Yb–N(2$^\#$)	2.403(14)	Yb–N(2)	2.403(14)
Yb–N(1$^\#$)	2.43(4)	Yb–N(1)	2.43(4)
Yb–C(15$^\#$)	3.08(2)	Yb–C(15)	3.08(2)
Yb–C(5)	3.14(2)	Yb–C(5$^\#$)	3.14(2)
Yb–C(6$^\#$)	3.16(2)	Yb–C(6)	3.16(2)
C(1)–C(4)	1.53(4)	C(2)–C(4)	1.51(3)
C(3)–C(4)	1.48(4)	C(4)–N(1)	1.37(5)
N(1)–C(6)	1.61(6)	C(5)–C(6)	1.39(3)
C(5)–N(2)	1.51(6)	N(2)–C(7)	1.40(3)
C(7)–C(9)	1.49(3)	C(7)–C(8)	1.51(3)
C(7)–C(10)	1.52(3)	C(11)–C(14)	1.50(3)
C(12)–C(14)	1.53(3)	C(13)–C(14)	1.53(3)
C(14)–N(3)	1.38(5)	N(3)–C(15)	1.54(6)
C(15)–C(15$^\#$)	1.35(4)		

Table 4
Bond angles [°]. Symmetry transformations used to generate equivalent atoms: ($^\#$: −x, y, −z)

sAtoms, Angle		Atoms	Angle	
N(3$^\#$)–Yb–N(3)	84(3)	N(3$^\#$)–Yb–N(2)#1	102(2)
N(3)–Yb–N(2$^\#$)	79(2)	N(3$^\#$)–Yb–N(2)	79(2)
N(3)–Yb–N(2)	102(2)	N(2$^\#$)–Yb–N(2)	179(3)
N(3$^\#$)–Yb–N(1$^\#$)	174(3)	N(3)–Yb–N(1$^\#$)	100.1(7)
N(2$^\#$)–Yb–N(1$^\#$)	83(2)	N(2)–Yb–N(1$^\#$)	96(2)
N(3$^\#$)–Yb–N(1)	100.1(7)	N(3)–Yb–N(1)	174(3)
N(2$^\#$)–Yb–N(1)	96(2)	N(2)–Yb–N(1)	83(2)
N(1$^\#$)–Yb–N(1)	76(3)	N(3$^\#$)–Yb–C(15$^\#$)	29.5(13)
N(3)–Yb–C(15$^\#$)	54.8(13)	N(2$^\#$)–Yb–C(15$^\#$)	93(2)
N(2)–Yb–C(15$^\#$)	88(2)	N(1$^\#$)–Yb–C(15$^\#$)	154.9(14)
N(1)–Yb–C(15$^\#$)	129.5(14)	N(3$^\#$)–Yb–C(15$^\#$)	54.9(13)
N(3)–Yb–C(15)	29.5(13)	N(2$^\#$)–Yb–C(15)	88(2)
N(2)–Yb–C(15)	93(2)	N(1$^\#$)–Yb–C(15)	129.5(14)
N(1)–Yb–C(15)	154.9(14)	C(15$^\#$)–Yb–C(15)	25.4(7)
N(3$^\#$)–Yb–C(5)	83.8(14)	N(3)–Yb–C(5)	129.3(13)
N(2$^\#$)–Yb–C(5)	151.7(12)	N(2)–Yb–C(5)	27.7(13)
N(1$^\#$)–Yb–C(5)	90.6(14)	N(1)–Yb–C(5)	55.2(14)
C(15$^\#$)–Yb–C(5)	103.8(5)	C(15)–Yb–C(5)	116.9(5)
N(3$^\#$)–Yb–C(5$^\#$)	129.3(13)	N(3)–Yb–C(5$^\#$)	83.8(14)
N(2$^\#$)–Yb–C(5$^\#$)	27.7(13)	N(2)–Yb–C(5$^\#$)	151.7(12)
N(1$^\#$)–Yb–C(5$^\#$)	55.2(14)	N(1)–Yb–C(5$^\#$)	90.6(14)
C(15$^\#$)–Yb–C(5$^\#$)	116.9(5)	C(15)–Yb–C(5$^\#$)	103.8(5)
C(5)–Yb–C(5$^\#$)	138.5(9)	N(3$^\#$)–Yb–C(6$^\#$)	154.7(13)
N(3)–Yb–C(6$^\#$)	88.5(14)	N(2$^\#$)–Yb–C(6$^\#$)	53.1(13)
N(2)–Yb–C(6$^\#$)	126.2(12)	N(1$^\#$)–Yb–C(6$^\#$)	30.1(14)
N(1)–Yb–C(6$^\#$)	85.9(14)	C(15$^\#$)–Yb–C(6$^\#$)	136.2(5)
C(15)–Yb–C(6$^\#$)	115.8(5)	C(5)–Yb–C(6$^\#$)	118.9(6)
C(5$^\#$)–Yb–C(6$^\#$)	25.5(6)	N(3$^\#$)–Yb–C(6)	88.5(14)
N(3)–Yb–C(6)	154.7(13)	N(2$^\#$)–Yb–C(6)	126.2(12)
N(2)–Yb–C(6)	53.1(13)	N(1$^\#$)–Yb–C(6)	85.9(14)
N(1)–Yb–C(6)	30.1(14)	C(15$^\#$)–Yb–C(6)	115.8(5)
C(15)–Yb–C(6)	136.2(5)	C(5)–Yb–C(6)	25.5(6)
C(5$^\#$)–Yb–C(6)	118.9(6)	C(6$^\#$)–Yb–C(6)	107.3(8)
N(1)–C(4)–C(3)	99(3)	N(1)–C(4)–C(2)	107(3)
C(3)–C(4)–C(2)	112(3)	N(1)–C(4)–C(1)	122(3)
C(3)–C(4)–C(1)	109(3)	C(2)–C(4)–C(1)	106(2)
C(4)–N(1)–C(6)	106(3)	C(4)–N(1)–Yb	150(3)
C(6)–N(1)–Yb	101(2)	C(6)–C(5)–N(2)	126(2)
C(6)–C(5)–Yb	78.3(12)	N(2)–C(5)–Yb	47.9(7)
C(5)–C(6)–N(1)	124(2)	C(5)–C(6)–Yb	76.3(11)
N(1)–C(6)–Yb	49(2)	C(7)–N(2)–C(5)	111(2)
C(7)–N(2)–Yb	144(3)	C(5)–N(2)–Yb	104(2)
N(2)–C(7)–C(9)	106(2)	N(2)–C(7)–C(8)	121(3)
C(9)–C(7)–C(8)	110(2)	N(2)–C(7)–C(10)	102(2)
C(9)–C(7)–C(10)	109(2)	C(8)–C(7)–C(10)	109(2)
N(3)–C(14)–C(11)	103(3)	N(3)–C(14)–C(13)	123(3)
C(11)–C(14)–C(13)	110(2)	N(3)–C(14)–C(12)	105(3)
C(11)–C(14)–C(12)	109(2)	C(13)–C(14)–C(12)	107(2)
C(14)–N(3)–C(15)	109(4)	C(14)–N(3)–Yb	147(3)
C(15)–N(3)–Yb	100(3)	C(15$^\#$)–C(15)–N(3)	127(2)
C(15$^\#$)–C(15)–Yb	77.3(4)	N(3)–C(15)–Yb	50(2)
Interplanar angles			
N1–C6–C5–N2		−12(5)	
N3–C15–C15$^\#$–N3$^\#$		−12(6)	

head mounted on a Syntex P2$_1$ diffractometer equipped with a low-temperature device. Lattice parameters were determined initially from the angular settings of 25 reflections and refined by a least-squared fit of 19 accurately centered reflections with $4° \leq 2\theta \leq 19°$. All intensity profiles were measured at 138(5) K and stored. The crystal data and some data collection parameters are given in Table 1. Three intensity control monitors were measured every 2 h of X-ray exposure time. The net intensities were corrected for decay and Lorentz and polarization effects. Analysis of the Patterson map revealed the location of the heavy atom. The positions of all non-hydrogen atoms were located on difference Fourier maps. Hydrogen atoms were introduced in calculated positions (d(C–H) = 96 pm [28], and refined with constant isotropic thermal parameter $U = 800$ pm^2. An empirical absorption correction (DIFABS [29] correction factor: min. 0.901, max. 1.194) was applied to the structure factors, and refinement proceeded with anisotropical thermal parameters for all non-hydrogen atoms by using blocked matrix least-squares methods. The final difference Fourier map showed no electron density greater than 1.1 or less than -0.602 e/ (10^6pm^3). X-ray scattering factors were taken from Cromer and Mann [30] and were corrected for anomalous dispersion [31]. Data reductions and all corrections were performed by using SHELX-93 [32].

The final atomic parameters are given in Table 2. Bond distances and angles are summarized in Tables 3 and 4. Further details of the structure investigation are available on request from the Fachinformationszentrum Karlsruhe, Gesellschaft für wissenschaftlich-technische Information mbH D-76344 Eggenstein-Leopoldshafen, Germany, upon quoting the depository number (CSD 401205), the authors names, and the full citation of the journal.

References

[1] G. van Koten and K. Vrieze, *Adv. Organomet. Chem., 21* (1982) 151.

[2] F.G.N. Cloke, H.C. de Lemos and A.A. Sameh, *J. Chem. Soc., Chem. Commun.*, (1986) 1344.

[3] A.A. Trifonov, A.V. Protchenko, V.K. Cherkasov and M.N. Bochkarev, *Metalloorg. Khim., 2* (1989) 471; *Organomet. Chem., USSR, 2* (1989) 237.

[4] M.N. Bochkarev, A.A. Trifonov, E.A. Fedorova, N.S. Emelyanova, T.A. Basalgina, G.S. Kalinina and G.A. Razuvaev, *J. Organomet. Chem., 372* (1989) 217.

[5] H. tom Dieck and H. Bruder, *J. Chem. Soc., Chem. Commun.*, (1977) 24.

[6] H. tom Dieck and A. Kinzel, *Angew. Chem., 91* (1979) 344; *Angew. Chem., Int. Ed. Engl., 18* (1979) 324.

[7] M. Svoboda, H. tom Dieck, C. Krüger and Y.H. Tsay, *Z. Naturforsch., 36b* (1981) 814.

[8] H. tom Dieck, M. Svoboda and T. Greiser, *Z. Naturforsch., 36b* (1981) 823.

[9] D. Walther, G. Kreisel and R. Kirmse, *Z. Anorg. Allgem. Chem., 487* (1982) 149.

[10] H. tom Dieck, R. Diercks, L. Stamp, H. Bruder and T. Schuld, *Chem. Ber., 120* (1987) 1943.

[11] H. tom Dieck, H.J. Rieger and G. Fendesak, *Inorg. Chim. Acta, 177* (1990) 191.

[12] (a) J.H. Van Vleck, *The Theory of Electronic and Magnetic Susceptibilities* Clarendon, Oxford, 1932; (b) E.M. Boudreaux and L.N. Mulay, *Theory and Application of Molecular Paramagnetism*, Wiley, New York, 1976.

[13] (a) D.J. Berg, C.J. Burns, R.A. Andersen and A. Zalkin, *Organometallics, 8* (1989) 1865; (b) D.J. Berg, *Ph.D. Thesis*, University of California, Berkeley, CA, 1987.

[14] A.L. Spek, PLUTON 92, University of Utrecht, 1992.

[15] C.K. Johnson, ORTEP, Report ORNL-3794, Oak Ridge National Laboratory, Tennessee, 1965.

[16] A.L. Wayda, J.L. Atwood and W.E. Hunter, *Organometallics, 3* (1984) 939.

[17] K.H. den Haan, J.L. de Boer, J.H. Teuben, A.L. Spek, B. Kojic-Prodic, G.R. Hays, R. Huis, *Organometallics, 5* (1986) 1726.

[18] H. Schumann, E. Palamidis and J. Loebel, *J. Organomet. Chem., 390* (1990) 45.

[19] T.D. Tilley, R.A. Andersen and A. Zalkin, *Inorg. Chem., 23* (1984) 2271.

[20] J.M. Boncella and R.A. Andersen, *Organometallics, 4* (1985) 205.

[21] M. Kaup, H. Stoll, H. Preuss, W. Kaim, T. Stahl, G. van Koten, E. Wissing, W.J.J. Smeets and A.L. Spek, *J. Am. Chem. Soc., 113* (1991) 5606.

[22] L.J.M. Huige, A.L. Spek and J.L. de Boer, *Acta Crystallogr., C41* (1985) 113.

[23] H. Schumann, P.R. Lee and J. Loebel, *Chem. Ber., 122* (1989) 1897.

[24] L. Pauling, *The Nature of the Chemical Bond*, New York, 2nd Ed., 1948.

[25] L.R. Chamberlain, L.D. Durfee, P.E. Fanwick, L.M. Kobriger, S.L. Latesky, A.K. McMullenm B.D. Steffey, I.P. Rothwell, K. Folting and J.C. Huffman, *J. Am. Chem. Soc., 109* (1987) 6068.

[26] F.G.N. Cloke, G.R. Hanson, M.J. Henderson, P.B. Hitchcock and C.L. Raston, *J. Chem. Soc., Chem. Commun.*, (1989) 1002.

[27] M. Veith and M. Bärninghausen, *Acta Crystallogr., B30* (1974) 1806.

[28] M.R. Churchill, *Inorg. Chem., 12* (1973) 1213.

[29] N. Walker and D. Stuart, *Acta Crystallogr., A39* (1983) 158.

[30] D. Cromer and J. Mann, *Acta Crystallogr., A24* (1968) 321.

[31] D. Cromer and D. Libermann, *J. Chem. Phys., 53* (1970) 1891.

[32] G.M. Sheldrick, SHELX-93, *Program for Crystal Structure Determination*, Universität Göttingen, 1993.